Solar Polarization 4
ASP Conference Series, Vol. 358, 2006
R. Casini and B. W. Lites

Supersonic Downflows in the Vicinity of a Solar Pore

A. Lagg, J. Woch, S. K. Solanki, and A. Gandorfer

Max-Planck-Institut für Sonnensystemforschung, Max-Planck-Strasse 2, D-37191 Katlenburg-Lindau, Germany

Abstract. At the footpoints of magnetic arcades spanning over a site of flux emergence we observe strong redshifts in the He I triplet at 1083 nm. These redshifts are associated with downflow speeds of up to $40\,\mathrm{km\,s^{-1}}$. Within the spatial resolution of our data ($1''$–$2''$) obtained with the Tenerife Infrared Polarimeter at the VTT we find an almost unshifted atmospheric component coexisting with the redshifted component. We were able to retrieve the magnetic field configuration in both the unshifted and the redshifted component simultaneously and infer an uncombed, fibril-like structure of the upper chromosphere. The supersonic downflow speeds are interpreted as a consequence of a significantly reduced pressure scale height above the pore, where the magnetic arcades are rooted. A temporal series of the fast downflow region reveals that the supersonic flow is maintained for more than one hour. Making use of the increased spatial resolution of the new TIP2 instrument we are working on reducing the upper limit on the size of the fibril-like flux channels in the upper chromosphere.

1. Introduction

Steady, high speed downflows are well known for transition region lines (e.g., Gebbie et al. 1981; Dere 1982; Teriaca, Banerjee, & Doyle 1999). At lower temperatures the velocities of the downflows generally decrease to a few $\mathrm{km\,s^{-1}}$. In arch filament systems or flaring regions downflows of up to $50\,\mathrm{km\,s^{-1}}$ have also been reported at chromospheric heights (e.g., Bruzek 1967; Teriaca et al. 2003), but only very recently spectroscopic observations of chromospheric high speed downflows are available (e.g., Schmidt, Muglach, & Knölker 2000). The processes responsible for such high flow velocities, usually lying above the local sound speed, are poorly understood. In this work we present a novel time series of spectro-polarimetric data in combination with a sophisticated analysis technique, possibly helping to shed some light onto the nature of chromospheric downflows.

2. Observations

An active region in the state of flux emergence was observed on May 13, 2001 in the upper chromospheric He I 1083 nm triplet with the Tenerife Infrared Polarimeter (TIP) mounted at the Vacuum Tower Telescope (VTT) on Tenerife, Canary Islands. The region (NOAA 9451) was seen under a viewing angle of $\cos\Theta \approx 0.8$ (solar coordinates: 33° W, 22° S). The magnetic topology of NOAA 9451 is discussed in Solanki et al. (2003), the analysis technique is described in

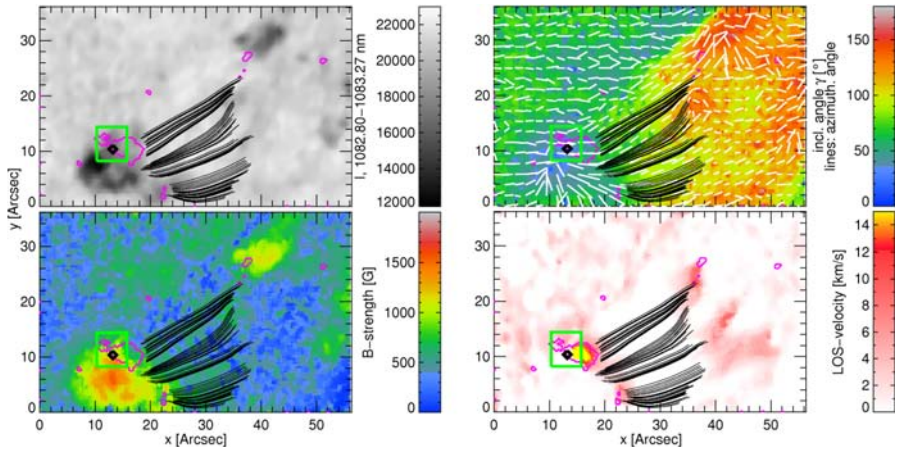

Figure 1. Continuum (top left), magnetic field strength (bottom left), magnetic field inclination (color-coded) and azimuth (white lines, top right), and velocity map (bottom right) of NOAA 9451. The temporal evolution was analyzed in the region enclosed by the green box. To increase the contrast the velocity map saturates at $15\,\mathrm{km\,s^{-1}}$ (the highest velocity values in the yellow region are $40\,\mathrm{km\,s^{-1}}$).

Lagg et al. (2004). Already during the observation we noticed large downflow velocities at one end of an Hα filamentary structure. We performed repetitive scans over this region enabling us to study the temporal evolution of this region, which turned out to be the footpoint of magnetic arcades spanning over a site of emergence of magnetic flux (Solanki et al. 2003). We obtained in total 11 snapshots, spanning a time interval of 73 min, where full Stokes vector polarimetry provided the information to obtain velocity and magnetic field maps. The spectral resolution was 29 mÅ per pixel, the spatial resolution was limited by the seeing to approximately 1.″5.

Figure 1 shows the maps of the observed region NOAA 9451 in line-of-sight coordinates. Clearly visible are the two pores located at the lower left and the upper right corner of the continuum image. The maps of the upper chromospheric magnetic field and the velocity were obtained by a two component inversion, only the component with the larger filling factor is shown. The field strength in the chromosphere reaches 1300 G in the trailing side of NOAA 9451 (lower left) and 900 G in the leading side. Magnetic loops span over the site of flux emergence (black lines). These loops have been calculated using the inclination and azimuth information retrieved from the Milne-Eddington type inversion technique described in the next section. A comparison of the observed loop structure with non-linear force-free magnetic field extrapolations using the photospheric maps showed a good agreement (Wiegelmann et al. 2005). The temporal analysis was performed for the area enclosed by the green rectangle.

3. Data Analysis

The spectral window contains two interesting lines: The He I 1083 nm triplet (effective Landé factors 2.0, 1.75, and 1.25), formed in the upper chromosphere,

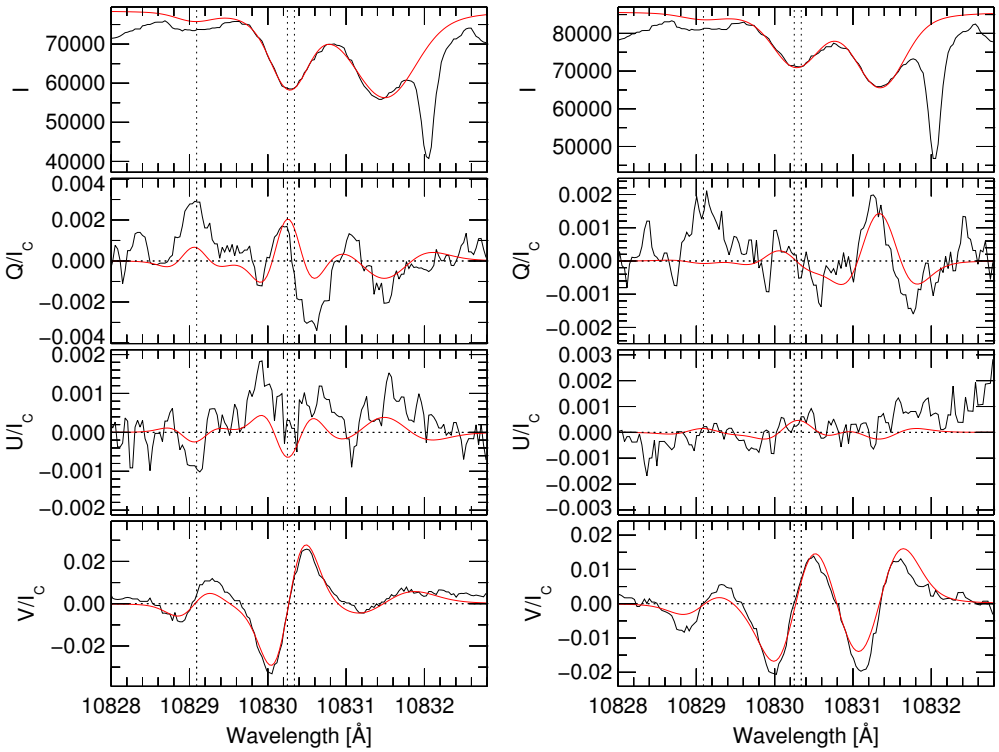

Figure 2. Stokes profiles for two different pixels showing two components. The central wavelengths of the He I triplet are indicated by the vertical, dashed lines. A second component of similar strength, red-shifted by ≈ 1 Å is clearly visible. Note that the magnetic properties of the two components are substantially different for the two profiles (compare the V profiles).

and the photospheric Si I 1082.7 nm line. The He I line was analyzed using a Milne-Eddington type inversion combined with the genetic algorithm PIKAIA (Charbonneau 1995). Details of the technique are described in Lagg et al. (2004). The method was extended to include the effects of the incomplete Paschen-Back regime (Socas-Navarro, Trujillo Bueno, & Landi Degl'Innocenti 2005; Sasso, Lagg, & Solanki 2005). The properties of the underlying photosphere were determined by the inversion code SPINOR (Frutiger et al. 2000). Both techniques are very robust in determining the best parameters describing the solar atmosphere within the assumed model. Especially the PIKAIA method turned out to be very effective in determining the accurate physical parameters regardless of the initial conditions.

Whereas for the majority of the pixels in the map presented in Fig. 1 a simple, one-component model is sufficient to obtain reasonable fits to the observed profiles, the Stokes profiles recorded at the footpoints of the magnetic arcades strongly indicate the presence of two independent components, shifted by velocities of up to 40 km s^{-1} (see Fig. 2). When the wavelength separation between the two components is large enough (> 10 km s^{-1}) and the filling factor for the minor component is larger than 20% an independent determination of the magnetic properties of the two components is possible. These pixels are marked by

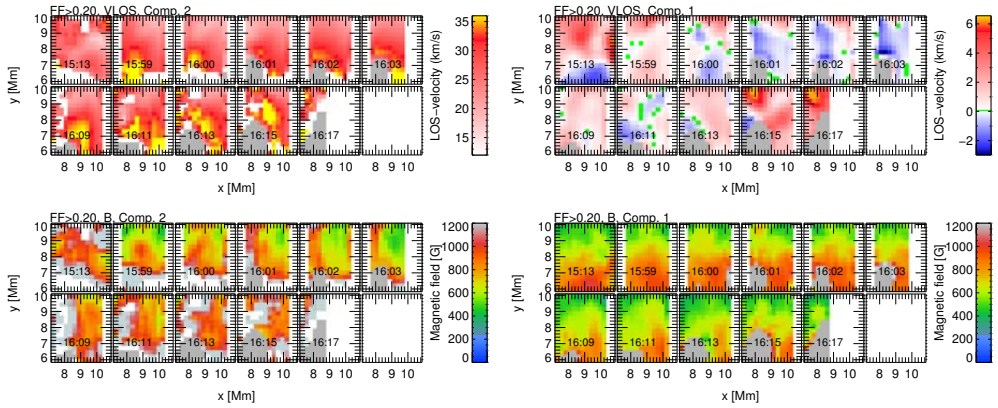

Figure 3. Temporal variation of LOS-velocity (left) and magnetic field strength (right) in the region of maximum downflow, for the fast component (top) and the slow component (bottom, see green rectangle in Fig. 1). The total time interval for the observations is 73 min. The area where the He I line goes into emission is marked in gray. Note the difference in velocity scale for the two components.

the areas enclosed by the magenta contour lines in Fig. 1. The two-component inversion improved the quality of the fit, determined by the difference between the observed and the synthetic profile, by 5 to 25%.

4. Downflow Properties

The analysis technique described above revealed maps of the physical parameters line-of-sight (LOS) velocity, magnetic field strength, inclination and azimuth for the two independent atmospheric components. These maps are presented in Figs. 3–4.

The fast downflow ($> 30\,\mathrm{km\,s^{-1}}$) in the upper chromosphere is evident over the whole time interval of our observations. Towards the end of this interval the area of the downflow region as well as the maximum velocities increase. Close to the region where the velocities reach values of more than $35\,\mathrm{km\,s^{-1}}$ the He I line goes into emission.[1] The slow component shows a larger relative variability: we observe downflows ($< 5\,\mathrm{km\,s^{-1}}$) and upflows ($< 3\,\mathrm{km\,s^{-1}}$).

Since PIKAIA looks for the absolute minimum in the χ^2 hypersurface and does not depend on the choice of the initial guesses, the fact that the inclination angle maps shown in Fig. 4 are relatively smooth suggests that this parameter is relatively reliably determined. The fast component (only shown if the filling factor exceeds 20%) is typically 10° to 40° more inclined to the LOS. The azimuthal angle is less reliably determined, since the polarization signal in Q and U is only in some pixels higher than the typical noise level. After the transformation to the solar reference frame, the fast component is again found to

[1] We exclude the emission profiles from our analysis. The pixels where the He I line goes into emission are plotted gray in the Figs. 3–4.

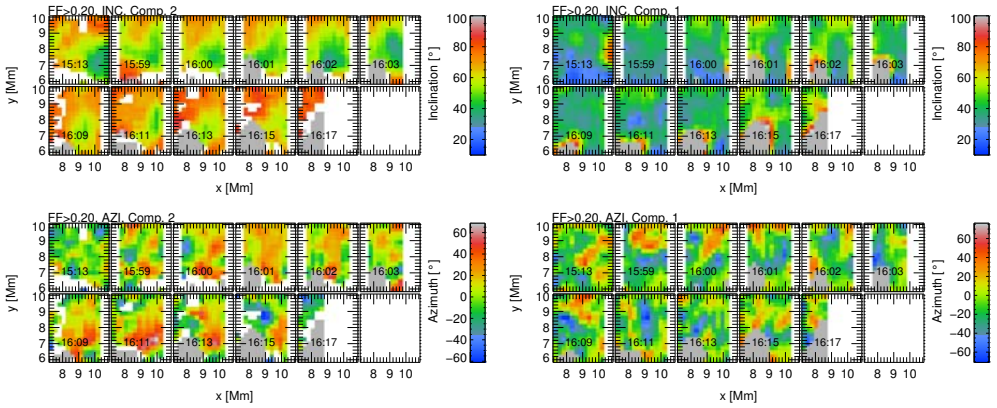

Figure 4. Same as Fig. 3 but for the magnetic field inclination (left) and azimuth (right) of the fast (top) and slow component (bottom). The same color scale is used for both components.

be more horizontal than the slow component by 10°–40°. The magnetic field strength for the slow component decreases slightly with time, whereas the field strength for the fast component undergoes stronger variations and is in general stronger than the field strength of the slow component.

The photosphere underlying this region of fast downflow initially shows a redshift of $\approx 0.6\,\mathrm{km\,s^{-1}}$ with respect to the quiet Sun (not shown). During the 73 min interval of observations the photospheric velocities increase by $\approx 0.7\,\mathrm{km\,s^{-1}}$, ending at around $1.3\,\mathrm{km\,s^{-1}}$. No significant temporal changes in other parameters, like magnetic field or Doppler broadening, are present in the photosphere.

5. Summary and Conclusion

The velocity of the downflowing material is significantly below the free fall speed, but lies above the sound speed, which is typically around $10\,\mathrm{km\,s^{-1}}$ at a height of 2 Mm, the "nominal" height of formation of the He I line. An attractive process to explain the observed downflows is related to the emergence of magnetic flux from the photosphere. Downflows in such regions can be explained as a result of the pressure balance between the rising flux tube and the surrounding atmosphere. As a consequence of the pressure balance, the flux tube has either to expand or to be emptied, the hydrostatic support of the material above is lost causing the material in the upper layers of the flux tube to drain to the solar surface. The general observed LOS structure corresponds well to this picture, with an upflow at the loop top. Without subsequent upward transport of material a loop would be emptied by drainage in about 20 min (Chou 1993). The upward transported, still cool material flows down along the field lines with higher downflow speeds towards the region with larger field strengths (i.e., lower gas pressure), which is the trailing side of NOAA 9451. This asymmetry is consistent with the observations by Spadaro et al. (2004).

We observe the highest downflow speeds near the edge of the trailing pore. We propose that this has to do with the cooling of the gas and the probable

concentration of the field, which happens in parallel. Both processes lower the gas pressure at a given height, the magnetic concentration by enhancing the Wilson depression, the cooling by decreasing the pressure scale height. Thus in the chromosphere the gas pressure can be an order of magnitude smaller than in the surrounding plage or quiet Sun. As a consequence the gas draining down from the rising cool loop can fall further until it hits upon stably stratified gas at a given pressure resulting in much larger velocities.

The different inclination angle of the two atmospheric components present in one resolution element points to an "uncombed" structure of the chromosphere. This indicates a similarity to the filamentary structure of the penumbra, namely that the chromospheric magnetic field is structured into flux-tube like structures, with a size less than the spatial resolution. Somewhat surprisingly the flux tubes containing the high-speed gas are usually more inclined than the flux tubes which are filled with material nearly at rest. This filamentary flux tube structure is stable over at least the duration of our observations.

References

Bruzek, A. 1967, Solar Phys., 2, 451
Charbonneau, P. 1995, ApJS, 101, 309
Chou, D.-Y. 1993, ASP Conf. Ser. Vol. 46, IAU Colloq. 141, ed. H. Zirin, G. Ai & H. Wang (San Francisco: ASP), 471
Dere, K. P. 1982, Solar Phys., 77, 77
Frutiger, C., Solanki, S. K., Fligge, M., & Bruls, J. H. M. J. 2000, A&A, 358, 1109
Gebbie, K. B., Hill, F., November, L. J., et al. 1981, ApJ, 251, L115
Lagg, A., Woch, J., Krupp, N., & Solanki, S. K. 2004, A&A, 414, 1109
Sasso, C., Lagg, A., & Solanki, S. K. 2005, in ESA SP-596, Proc.Intl.Sci.Conf. Chromospheric and Coronal Magnetic Fields, ed. D. E. Innes, A. Lagg, S. K. Solanki & D. Danesy (Noordwijk: ESA), CD
Schmidt, W., Muglach, K., & Knölker, M. 2000, ApJ, 544, 567
Socas-Navarro, H., Trujillo Bueno, J., & Landi Degl'Innocenti, E. 2005, ApJS, 160, 312
Solanki, S. K., Lagg, A., Woch, J., Krupp, N., & Collados, M. 2003, Nat, 425, 692
Spadaro, D., Billotta, S., Contarino, L., Romano, P., & Zuccarello, F. 2004, A&A, 425, 309
Teriaca, L., Banerjee, D., & Doyle, J. G. 1999, A&A, 349, 636
Teriaca, L., Falchi, A., Cauzzi, G., et al. 2003, ApJ, 588, 596
Wiegelmann, T., Lagg, A., Solanki, S. K., Inhester, B., & Woch, J. 2005, A&A, 433, 701